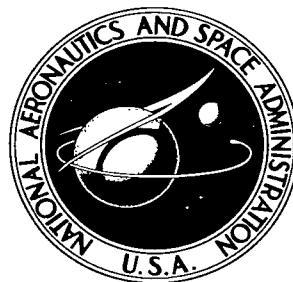


NASA TECHNICAL NOTE



NASA TN D-4158

e.1

LOAN COPY: RETURN
A. W. WILSON
KIRTLAND AFB, NM

0130710



NASA TN D-4158

INPUT ADMITTANCE OF A
COAXIAL TRANSMISSION LINE
OPENING ONTO A FLAT,
DIELECTRIC-COVERED GROUND PLANE

by Calvin T. Swift

Langley Research Center

Langley Station, Hampton, Va.



INPUT ADMITTANCE OF A COAXIAL TRANSMISSION LINE OPENING ONTO
A FLAT, DIELECTRIC-COVERED GROUND PLANE

By Calvin T. Swift

Langley Research Center
Langley Station, Hampton, Va.

NATIONAL AERONAUTICS AND SPACE ADMINISTRATION

For sale by the Clearinghouse for Federal Scientific and Technical Information
Springfield, Virginia 22151 - CFSTI price \$3.00

INPUT ADMITTANCE OF A COAXIAL TRANSMISSION LINE OPENING ONTO A FLAT, DIELECTRIC-COVERED GROUND PLANE

By Calvin T. Swift
Langley Research Center

SUMMARY

The input admittance of a coaxial transmission line opening onto a flat, dielectric-covered ground plane is derived, and computational results are given as a function of slab thickness in wavelengths. A dielectric constant of 2.57 was selected for the slab, which physically corresponds to that for lucite or polystyrene.

Surface wave contributions are considered in the calculations, and the results show that over some ranges of slab thickness 90 percent of the power supplied to the antenna is trapped in the dielectric.

Comments pertinent to a physically realizable antenna are included.

INTRODUCTION

In order to compute the input impedance of an antenna, a difficult electromagnetic boundary value problem must be solved. From a practical viewpoint, the problem should be solved either in rectangular, cylindrical, or spherical coordinates. This therefore requires a simple aperture and feed which can easily be described by these coordinates. The simplest example is that considered herein; that is, the large coaxial transmission line opening onto a flat ground plane, which can readily be described in cylindrical coordinates.

This antenna was originally investigated by Levine and Papas (ref. 1) who considered the same problem, with no dielectric cover. A variational expression for the admittance was derived which included the effects of higher order transmission-line modes on the admittance. Only the dominant mode was considered in the calculations, and the results compared favorably with the measured values of Hartig (ref. 2).

Later Galejs (ref. 3) treated the annular slot on a flat ground plane, feeding into a large circular waveguide containing a stratified plasma. By choosing a waveguide radius large compared to a wavelength, Galejs was able to infer the admittance of the coated slot on an infinitely large ground plane.

In this paper, as in reference 1, a flat ground plane of infinite area is initially assumed. The vector potential is written in terms of Hankel transforms and a three-region boundary value problem is then solved by assuming the existence of only the dominant transverse electromagnetic (TEM) mode at the aperture. Parseval's theorem is developed, which leads to an admittance expression containing an integral over the real axis in mode space, which must be numerically evaluated. Pole contributions in the integral are evaluated which physically describe surface wave propagation in the loss-free medium considered herein.

Numerical results are given as a function of dielectric slab thickness in wavelengths for a slab whose dielectric constant is 2.57.

SYMBOLS AND ABBREVIATIONS

Rationalized mks units are used for all calculations.

\vec{A}^*	magnetic vector potential
a	radius of inner conductor of transmission line
b	radius of outer conductor of transmission line or normalized input susceptance
\vec{E}	electric field intensity
g_r	normalized radiation conductance
g_s	normalized surface wave conductance
\vec{H}	magnetic field intensity
$j = \sqrt{-1}$	
$k = Nk_0$	
k_0	free-space wave number
k_z	axial wave number
N	index of refraction of slab

N'	index of refraction of dielectric in coaxial transmission line
P^*	complex conjugate of power
$R_n(\rho)$	general radial solution in the waveguide, $J_1(\lambda_n \rho) Y_0(\lambda_n a) - J_0(\lambda_n a) Y_1(\lambda_n \rho)$ where n is an integer ≥ 1
t	time
x, y, z	Cartesian coordinates
Y_0	characteristic admittance of free space, $\sqrt{\frac{\epsilon_0}{\mu_0}}$
Y_n	admittance of n th transmission-line mode, $\frac{jY_0 N'^2}{\sqrt{\left(\frac{\lambda_n}{k_0}\right)^2 - N'^2}}$
y_{in}	normalized input admittance
Z_c	characteristic impedance of coaxial transmission line, $\frac{1}{2\pi Y_0 N'} \ln \frac{b}{a}$
z_0	slab thickness
β	normalized radial mode number, ξ/k_0
β_n	location of surface wave pole in mode space
Γ	reflection coefficient
ϵ	permittivity
ϵ_0	permittivity of free space
λ_0	wavelength in free space
λ_n	cut-off wave number for higher order modes
λ_ϵ	wavelength in dielectric slab
μ_0	permeability of free space

ξ radial wave number
 ζ radial wave number used as dummy variable
 ρ, φ, z cylindrical coordinates
 ω angular frequency

Subscripts:

ρ, φ, z principal vector components in cylindrical coordinates
ap aperture

Superscripts:

0 within coaxial line
I in dielectric slab
II in free space
* complex conjugate except for vector potential

Abbreviations:

TEM transverse electromagnetic
TM transverse magnetic
VSWR voltage standing-wave ratio

A bar over a symbol indicates the Hankel transform. The letters PP before an integral indicate the principal part of the integral.

THEORY

A coaxial transmission line of inner radius a and outer radius b , as shown in figure 1, opens onto a conducting ground plane coated with dielectric material of

thickness z_0 . The line is excited in the dominant TEM mode and a time-harmonic field of the form $e^{-j\omega t}$ is assumed. Since the fields are symmetric in φ and TEM to z inside the guide, the only nonvanishing field components are H_φ , E_ρ , and E_z . As such, the fields may be developed from a magnetic vector potential consisting of only a φ -component. From Stratton (pp. 23-34 of ref. 4), this potential $A_\varphi^*(\rho, z)$ can be related to the field components as follows:

$$\left. \begin{aligned} H_\varphi(\rho, z) &= j\omega A_\varphi^*(\rho, z) \\ E_\rho(\rho, z) &= -\frac{1}{\epsilon} \frac{\partial A_\varphi^*(\rho, z)}{\partial z} \\ E_z(\rho, z) &= -\frac{1}{\epsilon} \frac{1}{\rho} \frac{\partial}{\partial \rho} [\rho A_\varphi^*(\rho, z)] \end{aligned} \right\} \quad (1)$$

where, for source-free homogeneous media, $A_\varphi^*(\rho, z)$ satisfies the Helmholtz equation

$$\frac{\partial^2 A_\varphi^*}{\partial \rho^2} + \frac{1}{\rho} \frac{\partial A_\varphi^*}{\partial \rho} + \frac{\partial^2 A_\varphi^*}{\partial z^2} + \left(k^2 - \frac{1}{\rho^2}\right) A_\varphi^* = 0 \quad (2)$$

The structure is unbounded in the radial direction; therefore, the solution to equation (2) is:

$$A_\varphi^*(\rho, z) = \int_0^\infty \overline{\xi A_\varphi^*}(\xi, z) J_1(\xi \rho) d\xi \quad (3)$$

where $\overline{A_\varphi^*}(\xi, z)$ is the Hankel transform of $A_\varphi^*(\rho, z)$, that is,

$$\overline{A_\varphi^*}(\xi, z) = \int_0^\infty \rho A_\varphi^*(\rho, z) J_1(\xi \rho) d\rho \quad (4)$$

The substitution of equation (3) into equation (2) reduces the Helmholtz equation to

$$\frac{d^2 \overline{A_\varphi^*}}{dz^2} + (k^2 - \xi^2) \overline{A_\varphi^*} = 0 \quad (5)$$

In free space ($z \geq z_0$), only outgoing traveling waves exist; therefore, this solution to equation (5) is

$$\overline{A_\varphi^*}(\xi, z) = C(\xi) e^{jk_z^{\text{II}} z} \quad (6)$$

where the roots of k_z^{II} must be chosen so that

$$k_z^{\text{II}} = k_0 \sqrt{1 - (\xi/k_0)^2} \quad (|\xi/k_0| < 1) \quad (7a)$$

$$k_z^{\text{II}} = jk_0 \sqrt{(\xi/k_0)^2 - 1} \quad (|\xi/k_0| > 1) \quad (7b)$$

Standing waves are supported within the homogeneous dielectric slab ($0 \leq z \leq z_0$); hence, this solution to equation (5) is

$$\overline{A}_\varphi^{*I}(\xi, z) = A(\xi)e^{jk_z^{\text{I}}z} + B(\xi)e^{-jk_z^{\text{I}}z} \quad (8)$$

where, for real index of refraction N , the branch of k_z^{I} is arbitrarily selected so that

$$k_z^{\text{I}} = k_0 \sqrt{N^2 - (\xi/k_0)^2} \quad (|\xi/k_0| < N) \quad (9a)$$

$$k_z^{\text{I}} = jk_0 \sqrt{(\xi/k_0)^2 - N^2} \quad (|\xi/k_0| > N) \quad (9b)$$

If $\overline{E}_{\rho, \text{ap}}(\xi)$ is defined as the unknown transform of the electric field at $z = 0$, the coefficients $A(\xi)$, $B(\xi)$, and $C(\xi)$ may be eliminated in preference to $\overline{E}_{\rho, \text{ap}}(\xi)$ by means of the boundary conditions at $z = 0$ and $z = z_0$; that is,

$$\left. \begin{aligned} \overline{H}_\varphi^{\text{II}}(\xi, z_0) &= \overline{H}_\varphi^{\text{I}}(\xi, z_0) \\ \overline{E}_\rho^{\text{II}}(\xi, z_0) &= \overline{E}_\rho^{\text{I}}(\xi, z_0) \\ \overline{E}_\rho^{\text{I}}(\xi, 0) &= \overline{E}_{\rho, \text{ap}}(\xi) \end{aligned} \right\} \quad (10)$$

By using equations (10) to solve for $A(\xi)$, $B(\xi)$, and $C(\xi)$, the transforms of the magnetic field in regions I and II may be obtained in the following form:

$$\overline{H}_\varphi^{\text{I}}(\xi, z) = \frac{k_0 N^2 \sqrt{\epsilon_0/\mu_0} \overline{E}_{\rho, \text{ap}}(\xi) \left[k_z^{\text{I}} \cos k_z^{\text{I}}(z - z_0) + jN^2 k_z^{\text{II}} \sin k_z^{\text{I}}(z - z_0) \right]}{k_z^{\text{I}} \left[N^2 k_z^{\text{II}} \cos k_z^{\text{I}} z_0 - jk_z^{\text{I}} \sin k_z^{\text{I}} z_0 \right]} \quad (11a)$$

and

$$\overline{H}_\varphi^{\text{II}}(\xi, z) = \frac{k_0 N^2 \sqrt{\epsilon_0/\mu_0} \overline{E}_{\rho, \text{ap}}(\xi) e^{jk_z^{\text{II}}(z - z_0)}}{N^2 k_z^{\text{II}} \cos k_z^{\text{I}} z_0 - jk_z^{\text{I}} \sin k_z^{\text{I}} z_0} \quad (11b)$$

The general solution of the fields inside the transmission line ($z < 0$) is a superposition of a forward propagating TEM mode plus all higher order of TM reflecting modes; that is,

$$E_{\rho}^0(\rho, z) = \frac{A_0}{\rho} \left[e^{jN'k_0z} + \Gamma e^{-jN'k_0z} \right] + \sum_{n=1}^{\infty} A_n R_n(\rho) e^{\sqrt{\lambda_n^2 - N'^2 k_0^2} z} \quad (12a)$$

$$H_{\varphi}^0(\rho, z) = \frac{N'Y_0 A_0}{\rho} \left[e^{jN'k_0z} - \Gamma e^{-jN'k_0z} \right] + \sum_{n=1}^{\infty} Y_n A_n R_n(\rho) e^{\sqrt{\lambda_n^2 - N'^2 k_0^2} z} \quad (12b)$$

where $R_n(\rho)$ is the radial solution and λ_n is the cut-off wave number of the n th higher order mode, as determined from the transcendental equation

$$J_0(\lambda_n a) Y_0(\lambda_n b) - Y_0(\lambda_n a) J_0(\lambda_n b) = 0 \quad (13)$$

which follows from the requirement that E_z must vanish at $\rho = a$ and $\rho = b$.

From the continuity of \bar{E}_{ρ} and \bar{H}_{φ} within the aperture a rigorous solution can be obtained for the unknowns $\bar{E}_{\rho, ap}(\xi)$, Γ , and A_n . However, for the present computations, it will be assumed that the quantity $\lambda_n^2 - k^2$ is large enough so that the sum of all higher order mode contributions is negligible ($A_1 = A_2 = \dots = A_n = 0$). Under this assumption, then, the internal fields at the aperture are

$$E_{\rho}^0(\rho, 0) = \frac{A_0}{\rho} (1 + \Gamma) \quad (14a)$$

$$H_{\varphi}^0(\rho, 0) = \frac{N'Y_0 A_0}{\rho} (1 - \Gamma) \quad (14b)$$

where Γ is the reflection coefficient.

Taking the transform of equation (14a) immediately yields

$$\bar{E}_{\rho, ap}(\xi) = A_0 (1 + \Gamma) \int_a^b J_1(\xi \rho) d\rho = -A_0 (1 + \Gamma) \frac{[J_0(\xi b) - J_0(\xi a)]}{\xi} \quad (15)$$

The complex conjugate of power flow out of the transmission line at $z = 0$, in terms of the field quantities in region 0, is given by

$$P^* = \frac{1}{2} \int_0^{2\pi} \int_a^b E_{\rho}^{0*}(\rho, 0) H_{\varphi}^0(\rho, 0) \rho d\rho d\varphi = \pi |A_0|^2 (1 + \Gamma^*) (1 - \Gamma) Y_0 N' \ln \frac{b}{a} \quad (16)$$

And, from Parseval's theorem (appendix A), the complex conjugate of power flow into region I, in terms of the field quantities in region I, is given by

$$\begin{aligned}
P^* &= \pi \int_0^\infty \bar{E}_{\rho,ap}^*(\xi) \bar{H}_\varphi(\xi,0) \xi d\xi \\
&= \pi k_0 N^2 Y_0 \int_0^\infty \frac{|\bar{E}_{\rho,ap}(\xi)|^2 \left[k_z^I \cos k_z^I z_0 - j N^2 k_z^II \sin k_z^I z_0 \right]}{k_z^I \left[N^2 k_z^II \cos k_z^I z_0 - j k_z^I \sin k_z^I z_0 \right]} \xi d\xi
\end{aligned} \tag{17}$$

Substituting explicitly for $\bar{E}_{\rho,ap}(\xi)$ (eq. (15)), and requiring continuity of power across the aperture results in

$$\begin{aligned}
y_{in} &= \frac{1 - \Gamma}{1 + \Gamma} \\
&= \frac{N^2}{N' \ln \frac{b}{a}} \int_0^\infty \frac{\left[1 - j \frac{N^2 \sqrt{1 - \beta^2}}{\sqrt{N^2 - \beta^2}} \tan(k_0 z_0 \sqrt{N^2 - \beta^2}) \right] \left[J_0(k_0 b \beta) - J_0(k_0 a \beta) \right]^2 d\beta}{\beta \sqrt{N^2 - \beta^2} \left[\frac{N^2 \sqrt{1 - \beta^2}}{\sqrt{N^2 - \beta^2}} - j \tan(k_0 z_0 \sqrt{N^2 - \beta^2}) \right]}
\end{aligned} \tag{18}$$

where $\beta = \xi/k_0$. Equation (18) is valid for complex N . For N real and greater than one, it is convenient to break up the integral in equation (18) as follows:

$$y_{in} = \frac{N^2}{N' \ln \frac{b}{a}} \left[\int_0^1 F_1(\beta) d\beta + \int_1^N F_2(\beta) d\beta + \int_N^\infty F_3(\beta) d\beta \right] \tag{19}$$

The choice of the phases of k_z^I and k_z^{II} (eqs. (9) and (7), respectively) requires that

$$F_1(\beta) = \frac{\left[1 - j \frac{N^2 \sqrt{1 - \beta^2}}{\sqrt{N^2 - \beta^2}} \tan(k_0 z_0 \sqrt{N^2 - \beta^2}) \right] \left[J_0(k_0 b \beta) - J_0(k_0 a \beta) \right]^2}{\beta \sqrt{N^2 - \beta^2} \left[\frac{N^2 \sqrt{1 - \beta^2}}{\sqrt{N^2 - \beta^2}} - j \tan(k_0 z_0 \sqrt{N^2 - \beta^2}) \right]} \tag{20a}$$

$$F_2(\beta) = \frac{-j \left[1 + \frac{N^2 \sqrt{\beta^2 - 1}}{\sqrt{N^2 - \beta^2}} \tan(k_0 z_0 \sqrt{N^2 - \beta^2}) \right] \left[J_0(k_0 b \beta) - J_0(k_0 a \beta) \right]^2}{\beta \sqrt{N^2 - \beta^2} \left[\frac{N^2 \sqrt{\beta^2 - 1}}{\sqrt{N^2 - \beta^2}} - \tan(k_0 z_0 \sqrt{N^2 - \beta^2}) \right]} \quad (20b)$$

$$F_3(\beta) = \frac{-j \left[1 + \frac{N^2 \sqrt{\beta^2 - 1}}{\sqrt{\beta^2 - N^2}} \tanh(k_0 z_0 \sqrt{\beta^2 - N^2}) \right] \left[J_0(k_0 b \beta) - J_0(k_0 a \beta) \right]^2}{\beta \sqrt{\beta^2 - N^2} \left[\frac{N^2 \sqrt{\beta^2 - 1}}{\sqrt{\beta^2 - N^2}} + \tanh(k_0 z_0 \sqrt{\beta^2 - N^2}) \right]} \quad (20c)$$

For the case of no coating ($z_0 = 0$)

$$N^2 F_1(\beta) = \frac{\left[J_0(k_0 b \beta) - J_0(k_0 a \beta) \right]^2}{\beta \sqrt{1 - \beta^2}} \quad (21a)$$

and

$$N^2 F_2(\beta) = N^2 F_3(\beta) = \frac{-j \left[J_0(k_0 b \beta) - J_0(k_0 a \beta) \right]^2}{\beta \sqrt{\beta^2 - 1}} \quad (21b)$$

which checks with the results of Levine and Papas (ref. 1).

The contour of integration of the integral (eq. (19)) is shown in figure 2. In addition to the branch point at $\beta = 1$, a finite number of poles exist on the real axis between $\beta = 1$ and $\beta = N$ as a result of nonconvergence of the Hankel transform for $A_\varphi^*(\rho, z)$. These poles are of order one, and they occur at the values of β for which the denominator of equation (20b) vanishes. These poles physically describe the launching of surface waves (i.e., energy which is confined within the dielectric coating). This represents real power and may be computed from πj times the residue of equation (20b). Thus the complete expression for the input admittance is

$$y_{in} = \frac{N^2}{N' \ln \frac{b}{a}} \left[\int_0^1 F_1(\beta) d\beta + PP \int_1^N F_2(\beta) d\beta + \int_N^\infty F_3(\beta) d\beta + \pi j \sum \text{Res} \right] \equiv g_r - jb + g_s \quad (22)$$

where g_r is the normalized radiation conductance, g_s is the normalized surface wave conductance, and b is the normalized susceptance. The PP preceding the integral of $F_2(\beta)$ denotes the principal part.

From appendix B, the expression for the surface wave conductance is given by

$$g_s = \frac{N^2}{N' \ln \frac{b}{a}} \pi j \sum \text{Res} = \frac{\pi N^2}{(k_0 z_0) N' \ln \frac{b}{a}} \sum_n \frac{[J_0(k_0 b \beta_n) - J_0(k_0 a \beta_n)]^2}{\beta_n^2 \left[1 + \frac{(N^2 - 1) \sin(2k_0 z_0 \sqrt{N^2 - \beta_n^2})}{(2k_0 z_0 \sqrt{N^2 - \beta_n^2})} \right]} \quad (23)$$

where β_n is the nth root of the denominator of equation (20b); that is,

$$\frac{N^2 \sqrt{\beta_n^2 - 1}}{\sqrt{N^2 - \beta_n^2}} - \tan(k_0 z_0 \sqrt{N^2 - \beta_n^2}) = 0 \quad (24)$$

It is to be noted that an onset of a surface wave mode occurs where $\beta_n = 1$ and the argument of the tangent is $0, \pi, 2\pi, \dots$, that is, where the thickness in wavelengths satisfies the equation

$$\frac{z_0}{\lambda_0} = \frac{n}{2\sqrt{N^2 - 1}} \quad (n = 0, 1, 2, \dots) \quad (25)$$

which is the same cut-off condition for TM plane waves propagating in a grounded dielectric sheet. It is of interest to note that the surface wave conductance becomes smaller as $k_0 b$ and $k_0 a$ become larger. This would be expected, because the radiation becomes more directive as the aperture size becomes large compared to a wavelength. If the dielectric slab contains a small amount of loss, the poles will be displaced slightly off the real axis, and thereby will give no residue contribution. The complex integrand of equation (18) will, however, be large in the vicinity of the poles and when integrated should give a conductance contribution close to that of g_s for the lossless slab.

As the losses increase, the poles and branch point will be far removed from the real axis, and the integrand of equation (18) will be a smooth function, presenting no problem for numerical evaluation.

RESULTS

Equation (22) was numerically evaluated on an IBM 7094 electronic data processing system. The Gaussian quadrature method was used to evaluate the integrals, and the surface wave conductance was evaluated separately by using equations (23) and (24).

A dielectric constant of 2.57 was selected for the exterior slab and 2.00 was selected for the material inside the line. The ratio of the radius of the outer conductor to the inner one b/a was taken to be 2.00. Nine values of $k_0 a$ were chosen in the

range $0.60 \leq k_0 a \leq 2.00$. For each value of $k_0 a$, admittance computations were performed as a function of z_0/λ_ϵ , where z_0 is the thickness of the slab and λ_ϵ is the wavelength in the dielectric slab. In the region $0 \leq \frac{z_0}{\lambda_\epsilon} \leq \frac{17}{32}$, the incremental values of z_0/λ_ϵ were $1/32$ and $1/16$ in the interval $\frac{3}{4} \leq \frac{z_0}{\lambda_\epsilon} \leq \frac{17}{16}$. Two additional calculations were performed at $\frac{z_0}{\lambda_\epsilon} = \frac{5}{8}$ and $\frac{23}{32}$. One surface wave pole exists for $0 \leq \frac{z_0}{\lambda_\epsilon} \leq 0.64$ and two poles exist for the remaining computations.

Plots of the input admittance as a function of slab thickness in wavelengths are shown in figure 3. For the smaller values of $k_0 a$, the radiation conductance is small and relatively constant over the entire range of dielectric thickness considered. However, as $k_0 a$ increases, the radiation conductance increases considerably and begins to vary periodically with slab thickness. It is of interest to note that, for thicknesses beyond a quarter-wavelength, maximums and minimums occur at roughly every quarter-wavelength of slab thickness.

The surface wave conductance shows no general periodic behavior with slab thickness. It is of interest to note that the surface wave conductance can be appreciable for relatively small values of $k_0 a$, as shown in figure 3(a). For $k_0 a = 0.595$, over 90 percent of the power supplied to the aperture can be trapped within the dielectric layer. On the other hand, for some combinations of $k_0 a$ and nonzero slab thicknesses, the surface wave conductance is negligible. In particular, at $k_0 a = 1.800$, there is essentially no trapping in the range $0.4 < \frac{z_0}{\lambda_\epsilon} < 0.6$.

The capacitance of the antenna initially rises with increasing slab thickness, oscillates, and the susceptance actually becomes inductive over a range of thicknesses for $k_0 a$ greater than 1.305.

The admittance for the case where the external medium is a half-space of dielectric constant $\epsilon/\epsilon_0 = 2.57$ (i.e., $z_0 = \infty$) is indicated in figure 3 for the first few values of $k_0 a$. It can be seen that extremely thick slabs are required for the admittance to approach that of an infinite half-space.

As a partial check, the no-coating calculations ($z_0 = 0$) are compared with those of reference 1 in figure 4 for $b/a = 1.57, 2.00, \text{ and } 2.36$. The results generally agree; however, there is some discrepancy which is probably due to small errors in the manual procedure used in reference 1 to evaluate the integrals numerically. This supposition seems to be supported by the more recent calculations of Curtis (ref. 5).

DISCUSSION

Results have been plotted as a function of thickness in wavelengths to demonstrate the gross changes that can occur in the admittance after a reentry vehicle has partially ablated. The dielectric constant of 2.57, however, is not necessarily representative of that in ablation materials. This numerical value, $\epsilon/\epsilon_0 = 2.57$, was selected because it corresponds to that of lucite or polystyrene, both of which are commercially available in smooth sheets of sufficiently large area suitable for experiments at C-band and X-band frequencies. The loss tangents of lucite and polystyrene are also small enough at these frequencies to be considered negligible.

If experimental comparisons with the computations are performed, a few comments are appropriate. The results of figure 3 should first be cross-plotted to give admittance as a function of $k_0 a$ with a/z_0 as a constant parameter. This should be done because it is much more convenient, from the experimental viewpoint, to select a constant thickness and vary the frequency.

The dielectric constant of the material inside the line was taken as 2.00, which is close to that of teflon. Teflon was considered because it offers mechanical support and is a low-loss material which is relatively easy to machine. If other dielectrics are required, the results must be adjusted by multiplying each value of the admittance by $\sqrt{\frac{2.00}{\epsilon/\epsilon_0}}$, where ϵ/ϵ_0 is the dielectric constant of the selected material. Care should be exercised to keep the value of $k_0 a$ below the cut-off frequency of the next higher order mode, as determined by equation (13).

The area of the ground plane and dielectric cover should be large enough to prevent the sudden termination from influencing the input admittance. The degree of influence of the slab and ground-plane terminations on the admittance can be ascertained by running a finger along the edges and noting any deflection of the VSWR meter. Circular slabs should be avoided because of a tendency of reflected power at the edge to be focused back into the aperture.

The aperture can probably best be fed by tapering or stepping the inner and outer conductors of a small commercial line up to the desired size, as discussed by Ragan (pp. 305-314 of ref. 6). However, it is doubtful that wide-band operation can be achieved. It is therefore suggested that admittance measurements be taken from a slot cut into the large transmission line, as was done by Hartig (ref. 2).

The variation in the characteristic impedance due to variations of the outer radius δb and of the inner radius δa is given by

$$\frac{\delta Z_c}{Z_c} = \frac{1}{\ln \frac{b}{a}} \left(\frac{\delta b}{b} - \frac{\delta a}{a} \right) \quad (26)$$

If the inner radius a is $3/8$ inch, then for $b/a = 2.00$, a variation of less than 1 percent can be expected in the characteristic impedance of the line if the tolerances in b and a are less than ± 0.002 inch. Tolerances in concentricity can usually be neglected if reasonable care has been exercised in the machine work (see p. 30-5 of ref. 7).

Calculations of the radiation patterns have not been included because it is doubtful that they could be reproduced experimentally except for those thicknesses where the surface wave conductance is negligible. If the structure is curved or terminated, that power which is theoretically a surface wave on an infinite structure will be released into the radiation field. Its interference with the computed pattern can usually be discussed only in a qualitative manner.

CONCLUDING REMARKS

The input admittance of a coaxial transmission line opening onto a flat, dielectric-covered ground plane is derived, and computational results are given as a function of slab thickness in wavelengths. A dielectric constant of 2.57 was selected for the slab, which physically corresponds to that for lucite or polystyrene.

Surface wave contributions are considered in the calculations, and the results show that over some ranges of slab thickness 90 percent of the power supplied to the antenna is trapped in the dielectric.

Comments pertinent to a physically realizable antenna are included.

Langley Research Center,
National Aeronautics and Space Administration,
Langley Station, Hampton, Va., March 23, 1967,
129-01-03-03-23.

APPENDIX A

PARSEVAL'S THEOREM FOR HANKEL TRANSFORMS

From equation (16), the complex conjugate of power radiated by the aperture can be given by

$$P^* = \pi \int_a^b \mathbf{E}_{\rho, \text{ap}}^*(\rho, 0) \mathbf{H}_{\varphi}^I(\rho, 0) \rho \, d\rho \quad (\text{A1})$$

If equation (A1) is used directly in the computation of the aperture admittance, two integrations are required. First, the transform $\bar{\mathbf{H}}_{\varphi}^I(\xi, 0)$ must be integrated over all modes ξ to obtain $\mathbf{H}_{\varphi}^I(\rho, 0)$. Then the integration over ρ must be performed in accordance with equation (A1). Parseval's theorem reduces the problem to a single integration.

To develop Parseval's theorem for Hankel transforms, first let

$$\left. \begin{aligned} \mathbf{E}_{\rho, \text{ap}}^I(\rho, 0) &= \int_0^{\infty} \xi \bar{\mathbf{E}}_{\rho, \text{ap}}^I(\xi, 0) J_1(\xi\rho) \, d\xi \\ \mathbf{H}_{\varphi}^I(\rho, 0) &= \int_0^{\infty} \xi \bar{\mathbf{H}}_{\varphi}^I(\xi, 0) J_1(\xi\rho) \, d\xi \end{aligned} \right\} \quad (\text{A2})$$

Then substituting equations (A2) into equation (A1) and interchanging the order of integration gives

$$P^* = \pi \int_0^{\infty} \int_0^{\infty} d\xi \, d\xi \xi \bar{\mathbf{E}}_{\rho}^I(\xi, 0) \bar{\mathbf{H}}_{\varphi}^I(\xi, 0) \left[\int_a^b J_1(\xi\rho) J_1(\xi\rho) \rho \, d\rho \right] \quad (\text{A3})$$

Since $\bar{\mathbf{E}}_{\rho}^I(\rho, 0)$ is zero on the ground plane, the integration on ρ can be extended from 0 to ∞ . The resulting equation is (eq. (5.22) of ref. 1)

$$\int_0^{\infty} J_1(\xi\rho) J_1(\xi\rho) \rho \, d\rho = \frac{\delta(\xi - \xi)}{\xi} \quad (\text{A4})$$

Hence, from the property of the Dirac delta function

$$P^* = \pi \int_0^{\infty} \xi \bar{\mathbf{E}}_{\rho}^I(\xi, 0) \bar{\mathbf{H}}_{\varphi}^I(\xi, 0) \, d\xi \quad (\text{A5})$$

Equation (A5) is Parseval's theorem for Hankel transforms.

APPENDIX B

DERIVATION OF THE SURFACE WAVE CONDUCTANCE

An inspection of the admittance integrands (eqs. (20a) to (20c)) will show that the denominator of equation (20b) can vanish for real β , specifically at those values $\beta = \beta_n$ which are the roots of the transcendental equation

$$\frac{N^2 \sqrt{\beta_n^2 - 1}}{\sqrt{N^2 - \beta_n^2}} - \tan(k_0 z_0 \sqrt{N^2 - \beta_n^2}) = 0 \quad (\text{B1})$$

It can further be shown that near $\beta = \beta_n$, the denominator behaves as $\beta - \beta_n$ and therefore represents a pole of order one.

For $1 \leq \beta \leq N$, the integrand $F_2(\beta)$ can be expressed in the form

$$F_2(\beta) = \frac{H(\beta)}{L(\beta)} = \frac{-jk_0 z_0}{\beta \kappa_e} \frac{[\kappa_e \cos \kappa_e + N^2 \kappa \sin \kappa_e] [J_0(k_0 b \beta) - J_0(k_0 a \beta)]^2}{[N^2 \kappa \cos \kappa_e - \kappa_e \sin \kappa_e]} \quad (\text{B2})$$

where, for convenience, κ and κ_e have been introduced so that

$$\left. \begin{aligned} \kappa &= \sqrt{\beta^2 - 1} k_0 z_0 \\ \kappa_e &= \sqrt{N^2 - \beta^2} k_0 z_0 \end{aligned} \right\} \quad (\text{B3})$$

and

$$L(\beta) = N^2 \kappa \cos \kappa_e - \kappa_e \sin \kappa_e \quad (\text{B4})$$

Since the poles are of order one, the integral of equation (B2) may be written

$$\int_1^N F_2(\beta) d\beta = \pi j \sum \text{Res}(\beta_n) + \text{PP} \int_1^N F_2(\beta) d\beta = \pi j \sum \frac{H(\beta_n)}{\left[\frac{d}{d\beta} L(\beta) \right]_{\beta=\beta_n}} + \text{PP} \int_1^N F_2(\beta) d\beta \quad (\text{B5})$$

APPENDIX B

The derivative of $L(\beta)$ at $\beta = \beta_n$ becomes

$$\left[\frac{dL(\beta)}{d\beta} \right]_{\beta=\beta_n} = \frac{\beta_n (k_0 z_0)^2}{\cos \kappa_{e,n}} \left[\frac{N^2}{\kappa_n} \cos^2 \kappa_{e,n} + \frac{\kappa_n N^2}{\kappa_{e,n}} \sin \kappa_{e,n} \cos \kappa_{e,n} + \frac{\sin \kappa_{e,n} \cos \kappa_{e,n}}{\kappa_{e,n}} + \cos^2 \kappa_{e,n} \right] \quad (\text{B6})$$

where κ_n and $\kappa_{e,n}$ are κ and κ_e , respectively, evaluated at $\beta = \beta_n$.

With the use of equation (B1), equation (B6) can be reduced to

$$\left[\frac{dL(\beta)}{d\beta} \right]_{\beta=\beta_n} = \frac{\beta_n (k_0 z_0)^2}{\cos \kappa_{e,n}} \left[1 + \left(\frac{N^2 - 1}{\beta_n^2 - 1} \right) \frac{\sin 2\kappa_{e,n}}{2\kappa_{e,n}} \right] \quad (\text{B7})$$

In terms of κ_n and $\kappa_{e,n}$, the numerator $H(\beta_n)$ is

$$H(\beta_n) = \frac{-j(k_0 z_0)}{\beta_n \kappa_{e,n}} \left[\kappa_{e,n} \cos \kappa_{e,n} + N^2 \kappa_n \sin \kappa_{e,n} \right] \left[J_0(k_0 a \beta_n) - J_0(k_0 b \beta_n) \right]^2 \quad (\text{B8})$$

And, again with the use of equation (B1), the preceding expression reduces to

$$H(\beta_n) = \frac{-jk_0 z_0 \left[J_0(k_0 b \beta_n) - J_0(k_0 a \beta_n) \right]^2}{\beta_n \cos \kappa_{e,n}} \quad (\text{B9})$$

Therefore, it follows that the surface wave conductance is

$$g_s = \frac{N^2}{N' \ln \frac{b}{a}} \pi j \sum \text{Res}(\beta_n) = \frac{\pi N^2}{k_0 z_0 N' \ln \frac{b}{a}} \sum_n \frac{\left[J_0(k_0 b \beta_n) - J_0(k_0 a \beta_n) \right]^2}{\beta_n^2 \left[1 + \left(\frac{N^2 - 1}{\beta_n^2 - 1} \right) \frac{\sin \left(2k_0 z_0 \sqrt{N^2 - \beta_n^2} \right)}{\left(2k_0 z_0 \sqrt{N^2 - \beta_n^2} \right)} \right]} \quad (\text{B10})$$

REFERENCES

1. Levine, Harold; and Papas, Charles H.: Theory of the Circular Diffraction Antenna. J. Appl. Phys., vol. 22, no. 1, Jan. 1951, pp. 29-43.
2. Hartig, Elmer O.: Circular Apertures and Their Effects on Half-Dipole Impedances. Ph.D. Thesis, Harvard Univ., 1950.
3. Galejs, Janis: Admittance of Annular Slot Antennas Radiating Into a Plasma Layer. AFCRL-63-395, AD 425 302, U.S. Air Force, Aug. 1963.
4. Stratton, Julius Adams: Electromagnetic Theory. McGraw-Hill Book Co., Inc., 1941.
5. Curtis, Walter L.: Calculated Values of Admittance for Annular Slot Antenna. D2-20301-1, The Boeing Co., Feb. 14, 1964. (Available from DDC as AD 469 612.)
6. Ragan, George L., ed.: Microwave Transmission Circuits. Dover Publ., Inc., 1965.
7. Jasik, Henry, ed.: Antenna Engineering Handbook. McGraw-Hill Book Co., Inc., 1961.

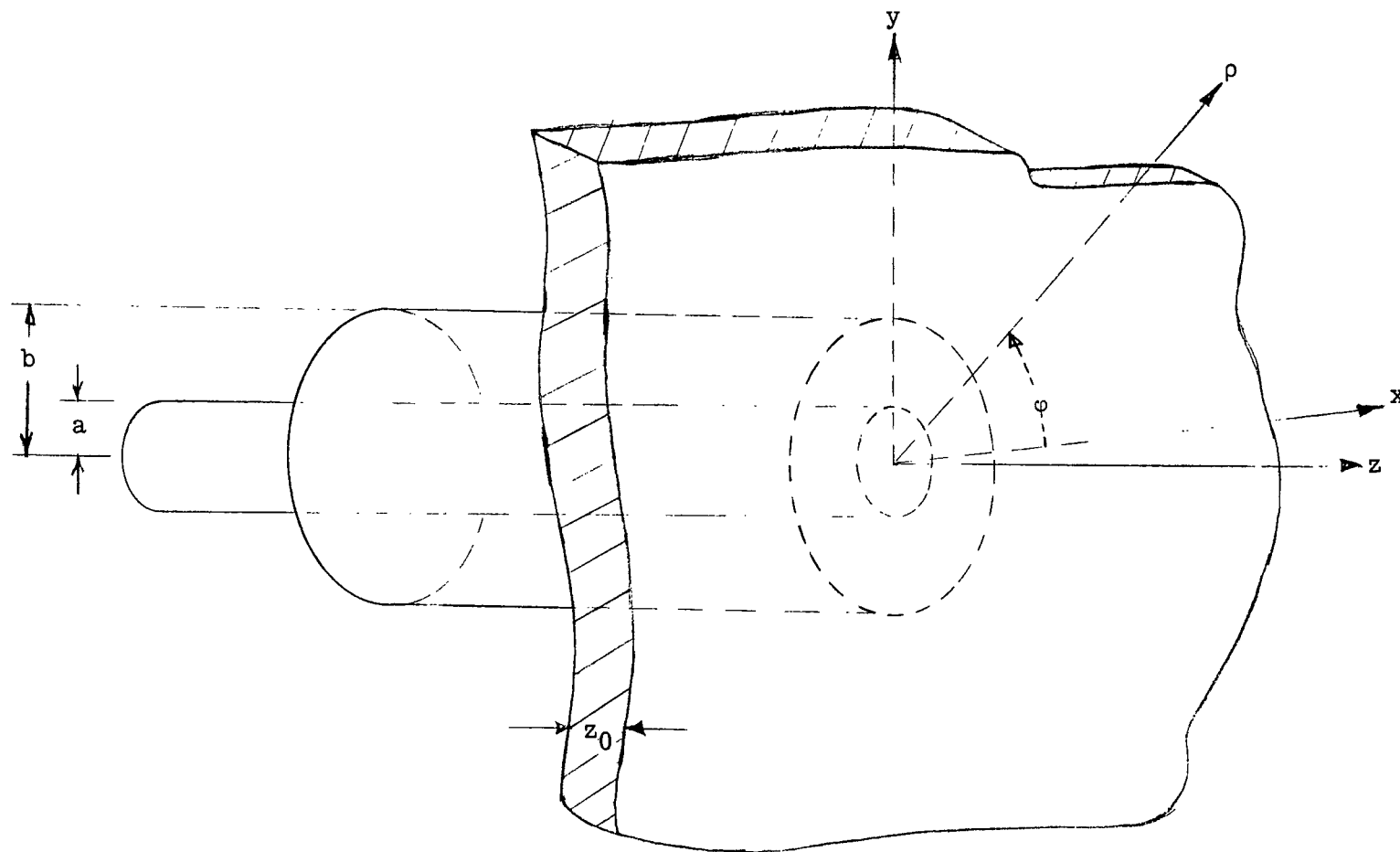


Figure 1.- Transmission-line antenna.

Im β

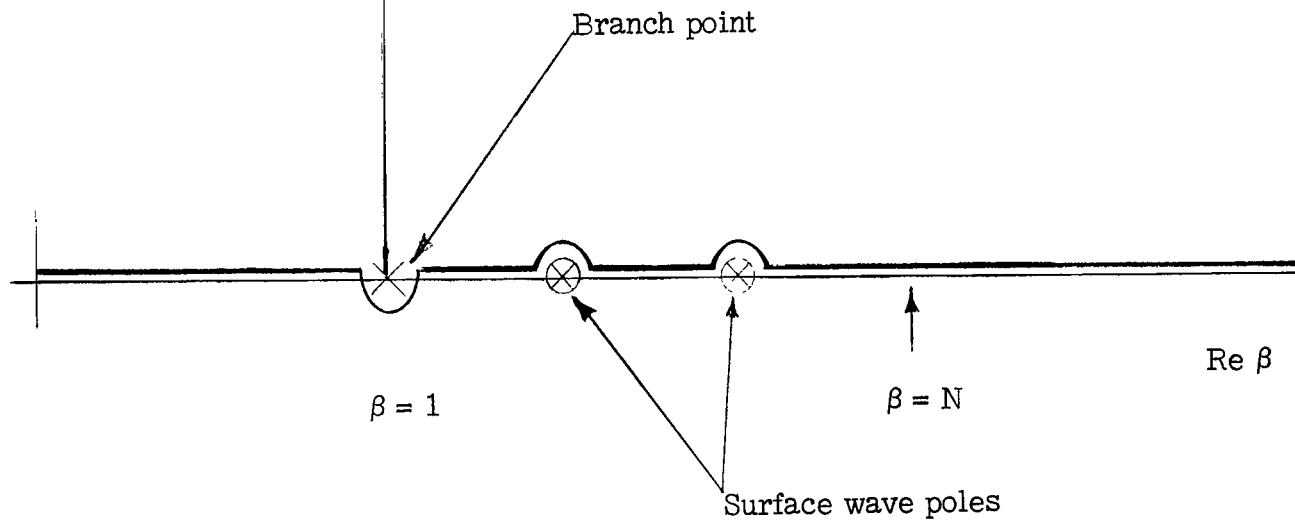
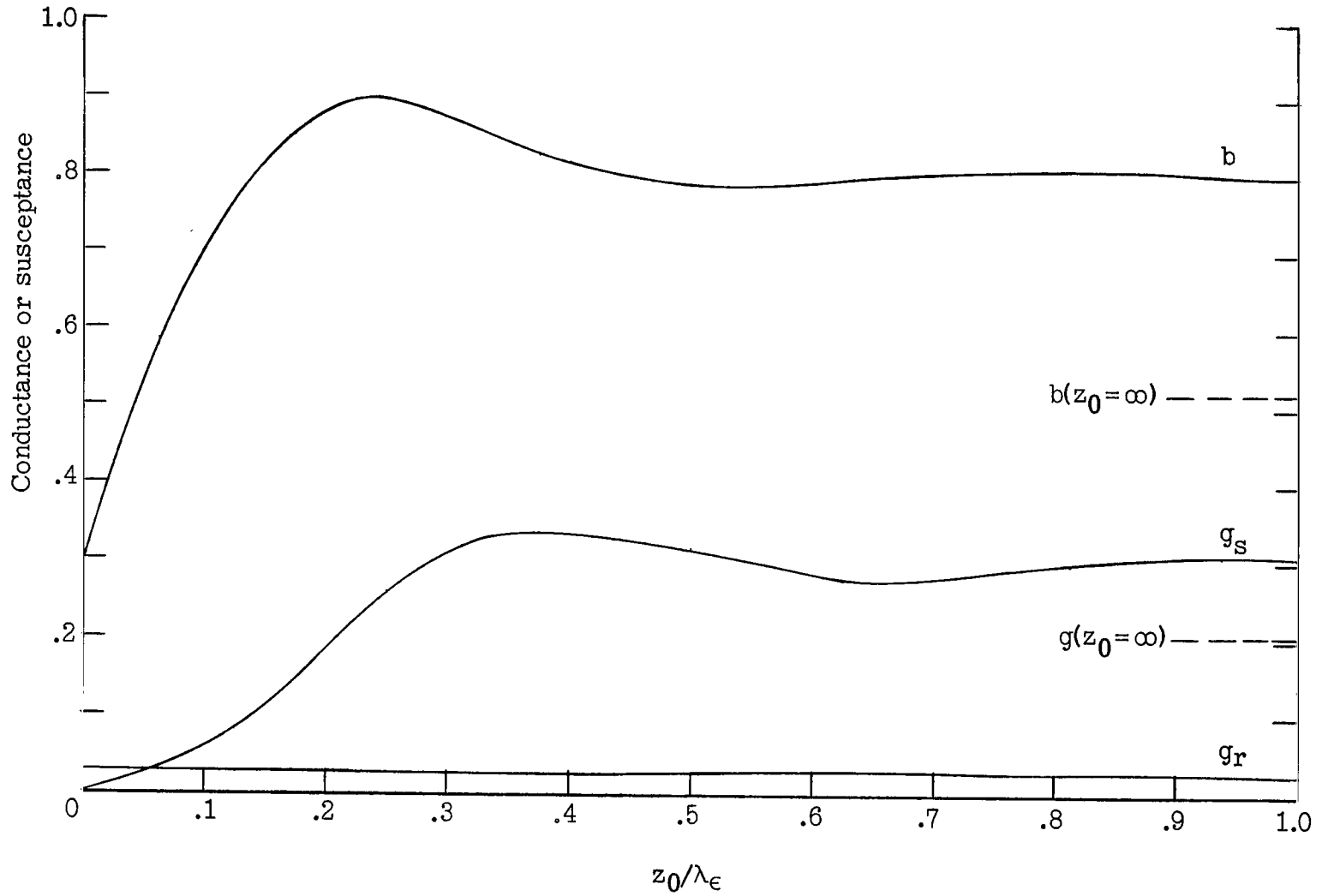
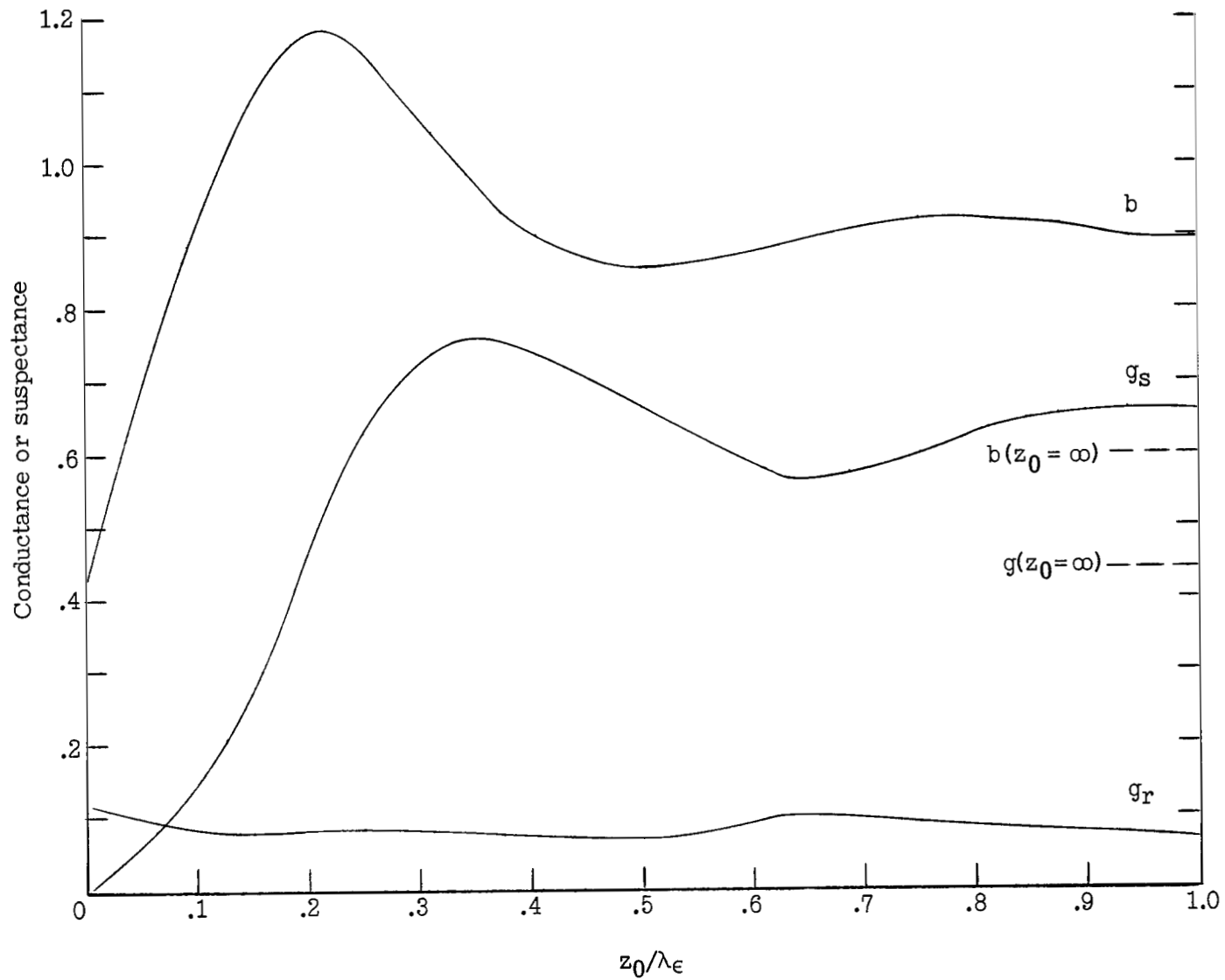


Figure 2.- Contour of integration in the complex β -plane.



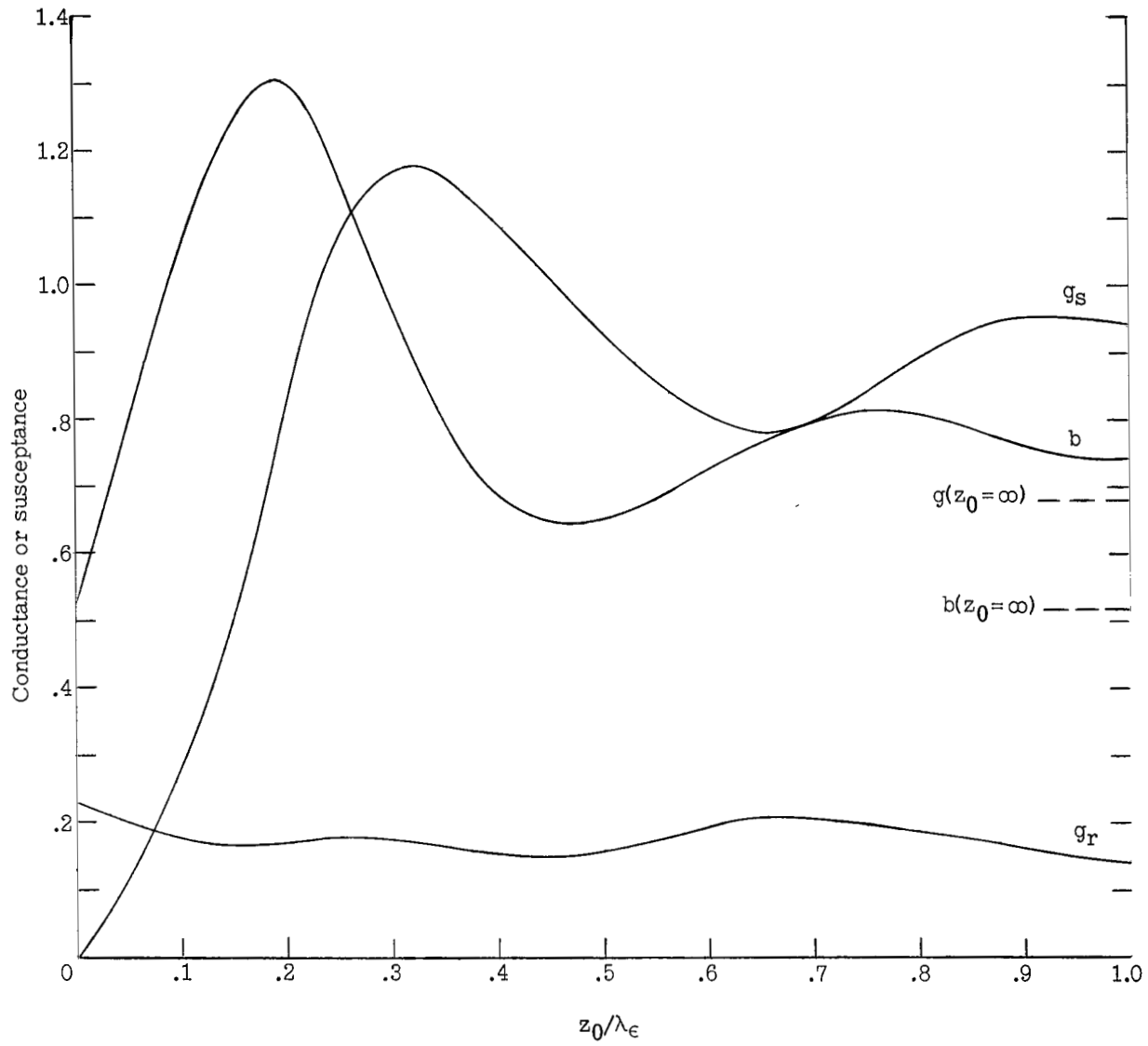
(a) $k_0 a = 0.595$.

Figure 3.- Input admittance as function of thickness in wavelengths. ($N' = 1.414$.)



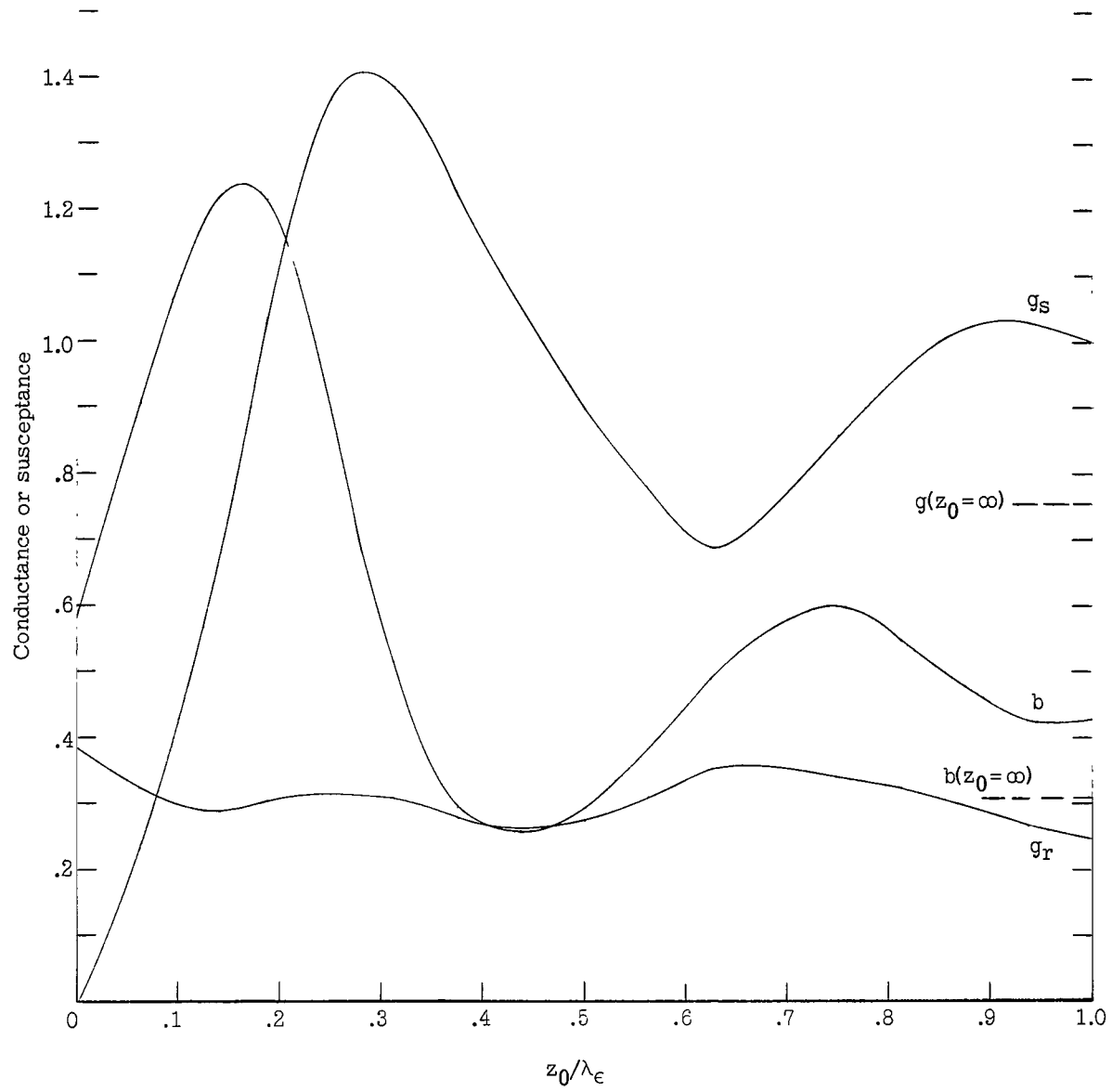
(b) $k_0 a = 0.800$.

Figure 3.- Continued.



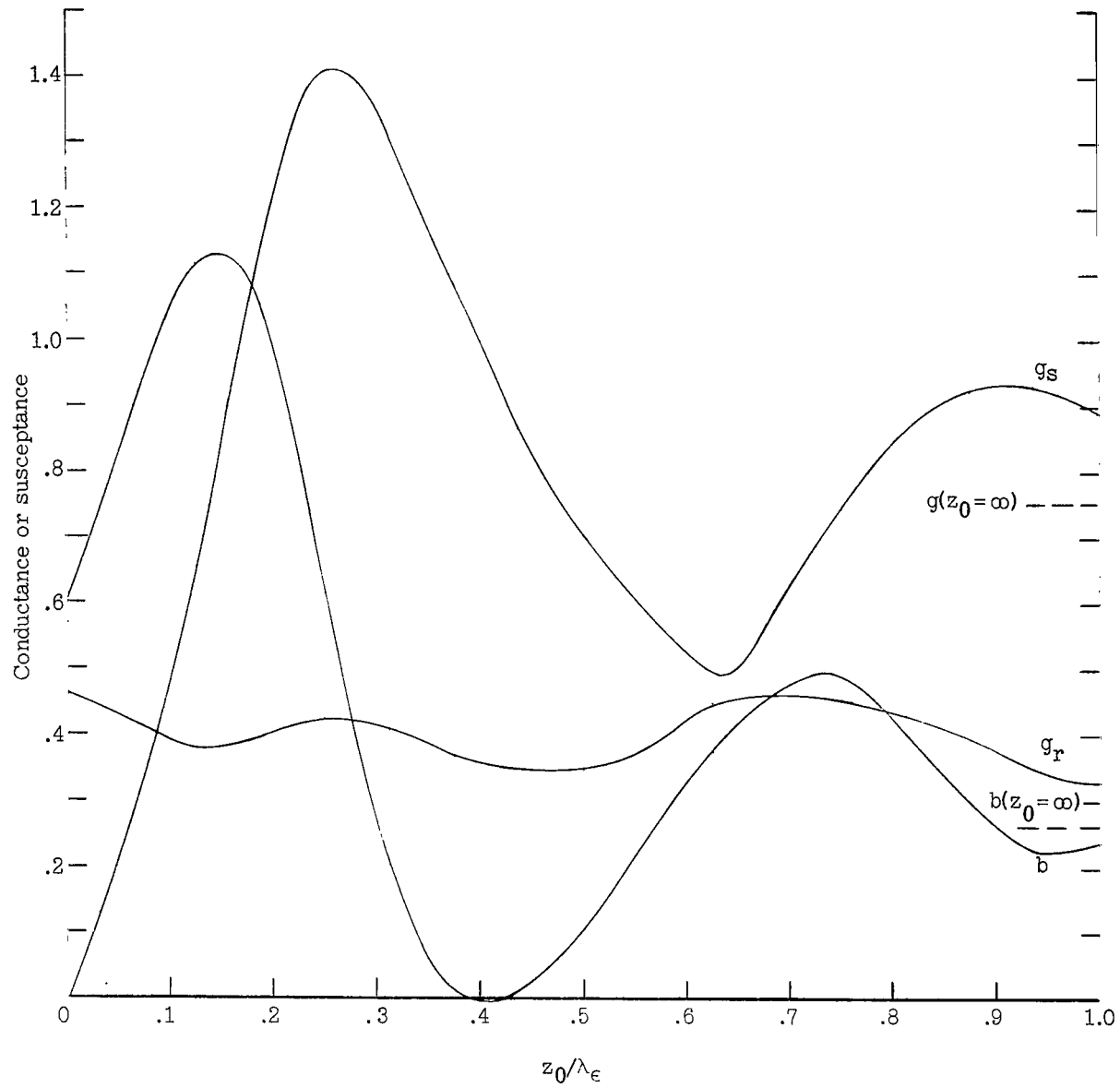
(c) $k_0 a = 0.995$.

Figure 3.- Continued.



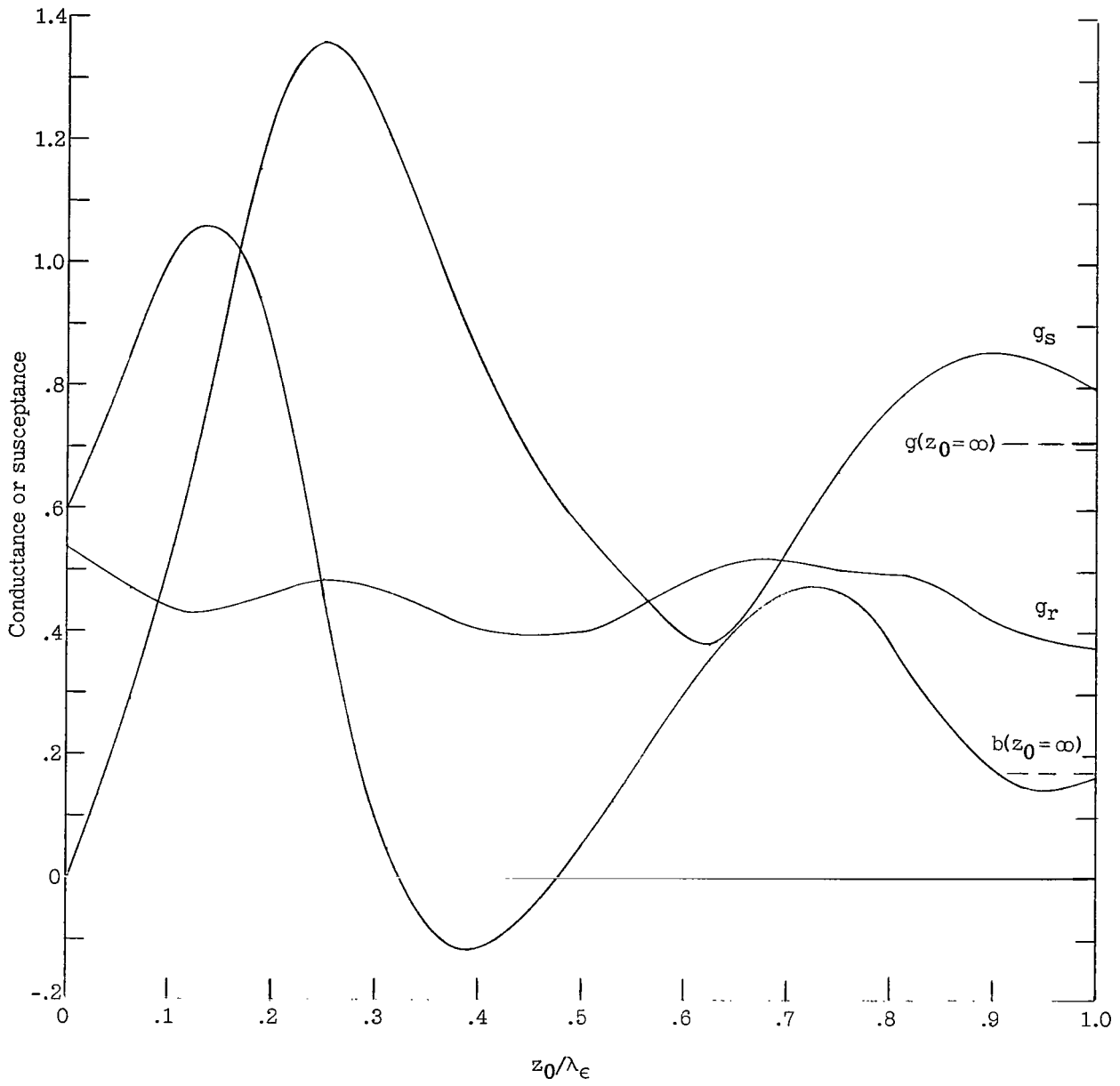
(d) $k_0 a = 1.200$.

Figure 3.- Continued.



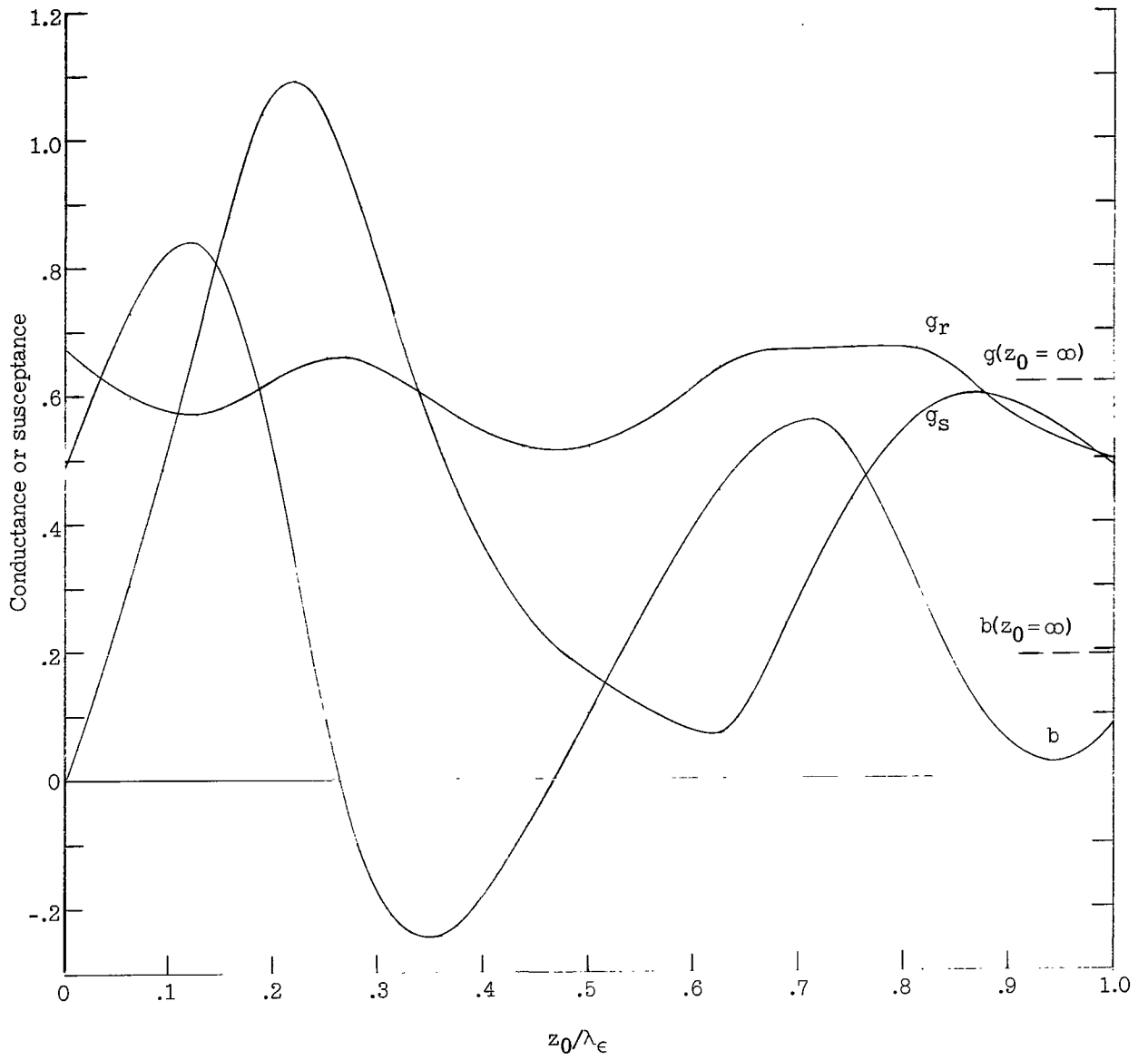
(e) $k_0 a = 1.305$.

Figure 3.- Continued.



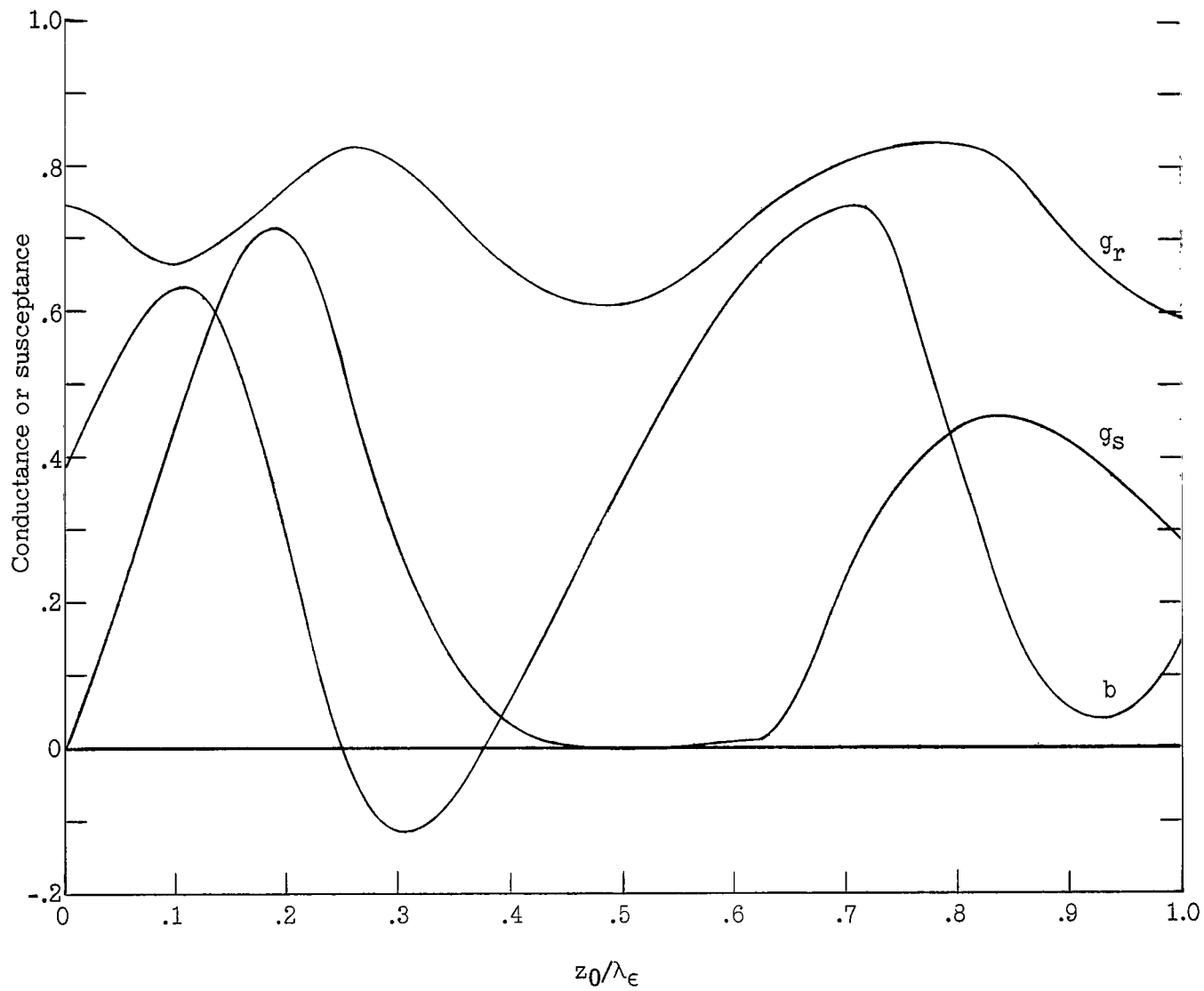
(f) $k_0 a = 1.397$.

Figure 3.- Continued.



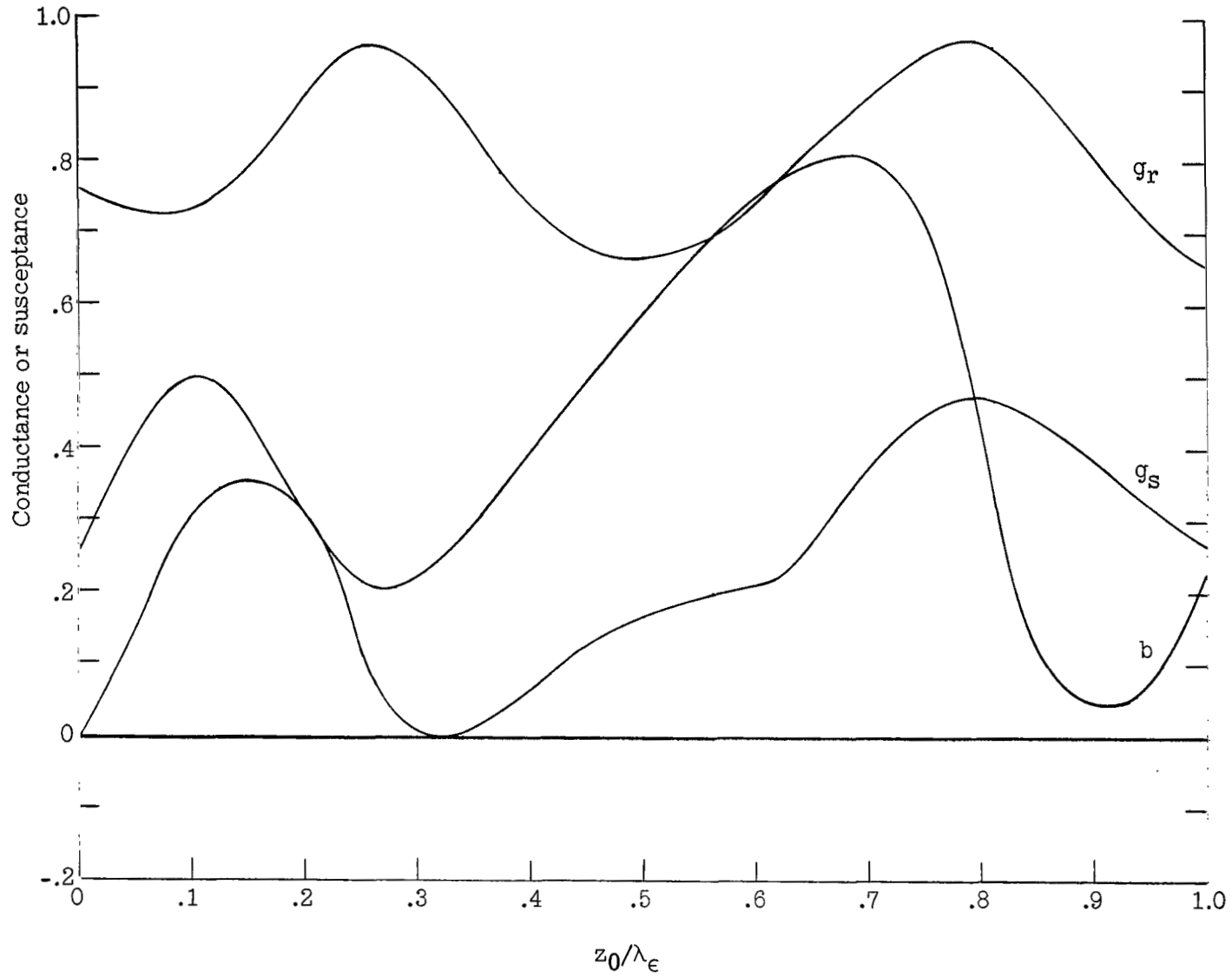
(g) $k_0 a = 1.600$.

Figure 3.- Continued.



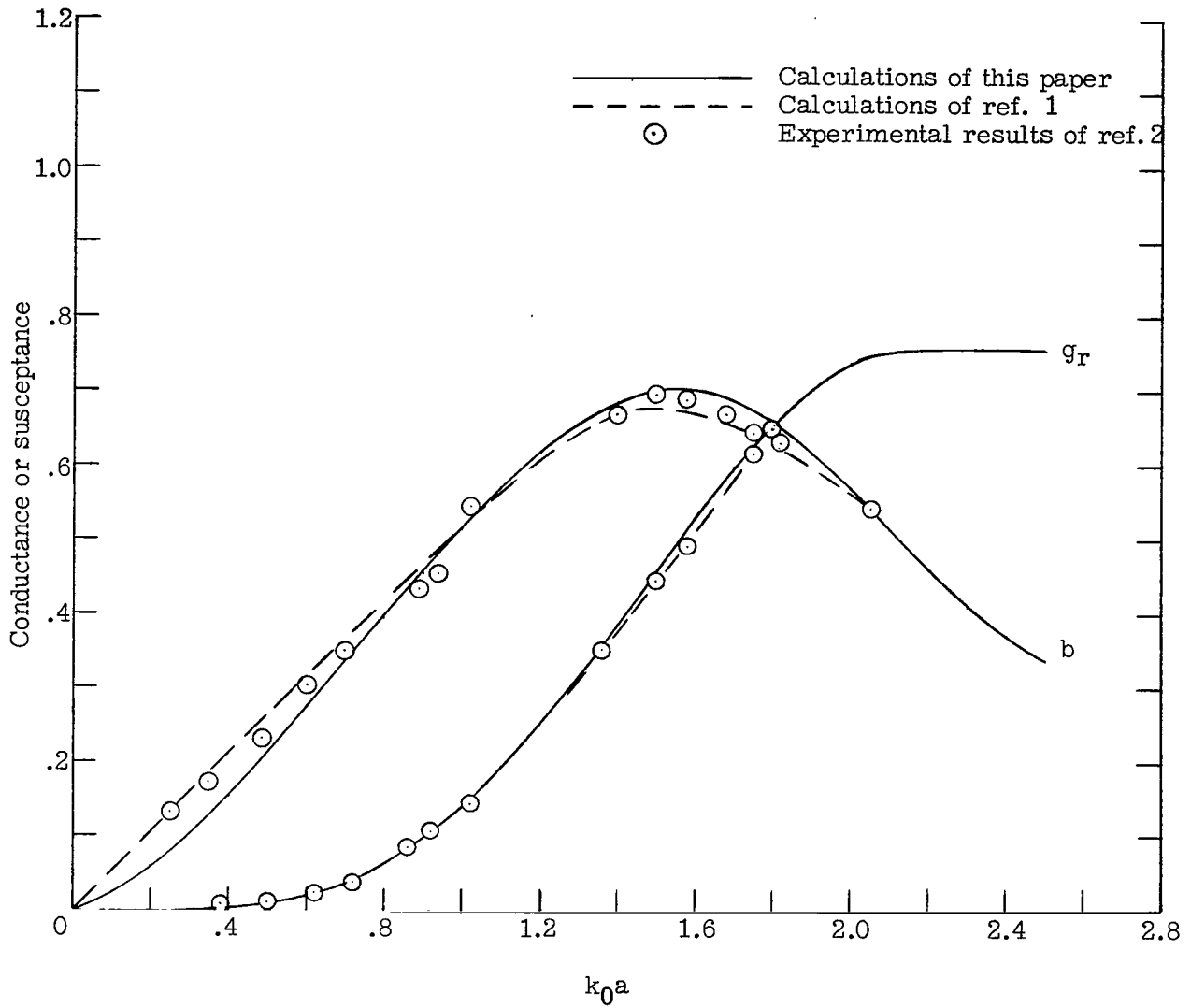
(h) $k_0 a = 1.800$.

Figure 3.- Continued.



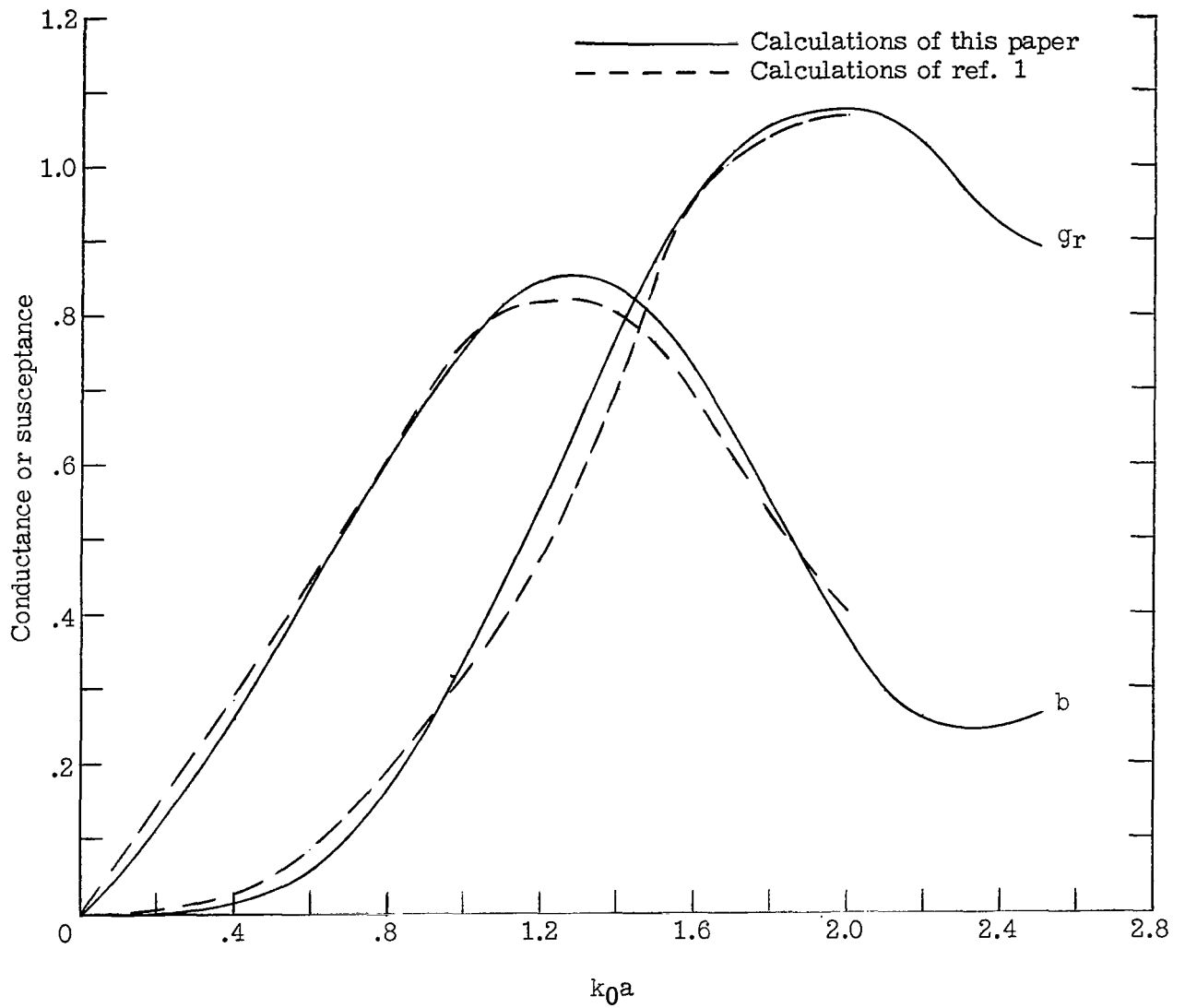
(i) $k_0a = 2.000$.

Figure 3.- Concluded.



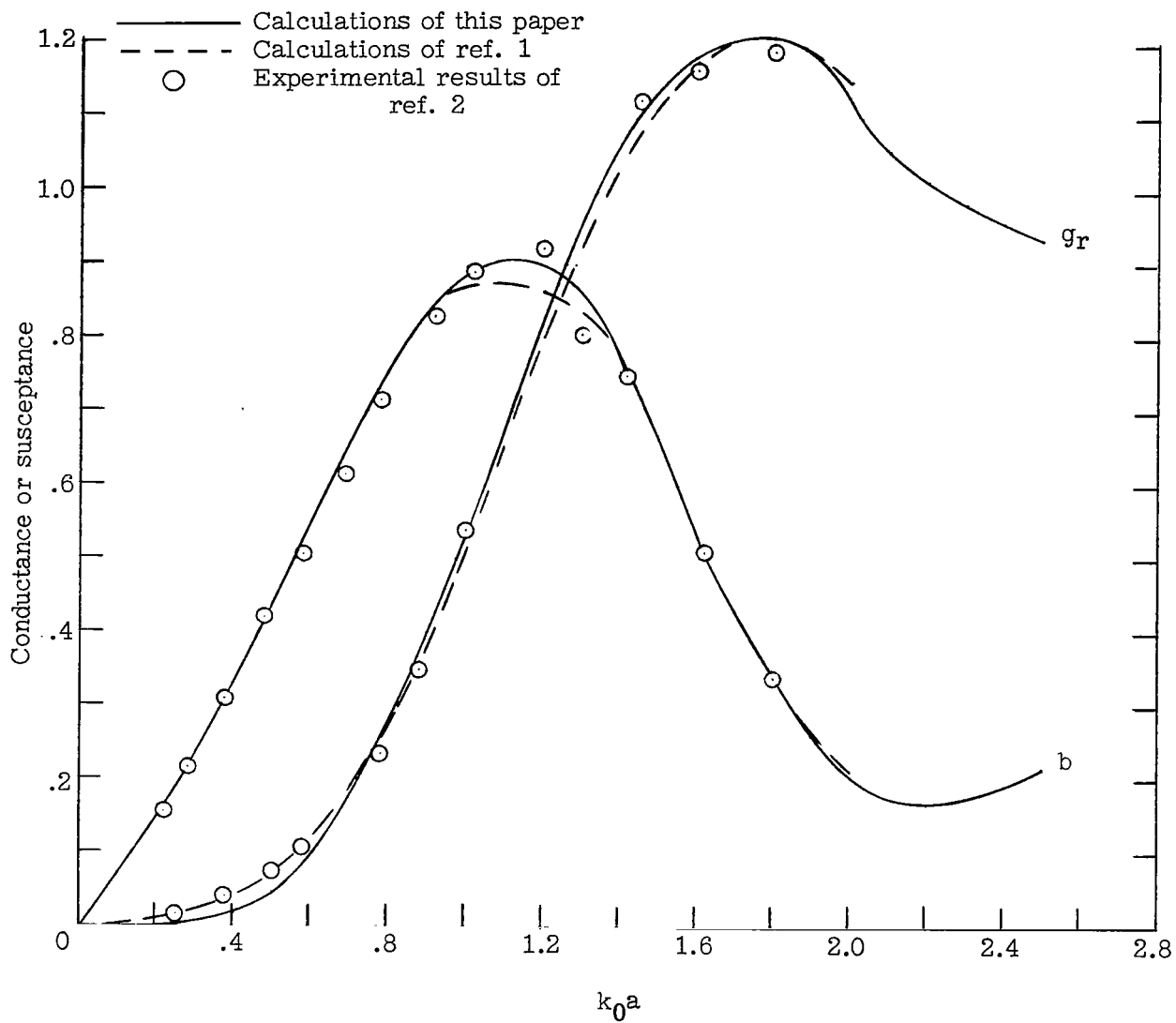
(a) $b/a = 1.57$.

Figure 4.- Input admittance as function of $k_0 a$. ($N' = 1$.)



(b) $b/a = 2.00$.

Figure 4.- Continued.



(c) $b/a = 2.36$.

Figure 4.- Concluded.

"The aeronautical and space activities of the United States shall be conducted so as to contribute . . . to the expansion of human knowledge of phenomena in the atmosphere and space. The Administration shall provide for the widest practicable and appropriate dissemination of information concerning its activities and the results thereof."

—NATIONAL AERONAUTICS AND SPACE ACT OF 1958

NASA SCIENTIFIC AND TECHNICAL PUBLICATIONS

TECHNICAL REPORTS: Scientific and technical information considered important, complete, and a lasting contribution to existing knowledge.

TECHNICAL NOTES: Information less broad in scope but nevertheless of importance as a contribution to existing knowledge.

TECHNICAL MEMORANDUMS: Information receiving limited distribution because of preliminary data, security classification, or other reasons.

CONTRACTOR REPORTS: Scientific and technical information generated under a NASA contract or grant and considered an important contribution to existing knowledge.

TECHNICAL TRANSLATIONS: Information published in a foreign language considered to merit NASA distribution in English.

SPECIAL PUBLICATIONS: Information derived from or of value to NASA activities. Publications include conference proceedings, monographs, data compilations, handbooks, sourcebooks, and special bibliographies.

TECHNOLOGY UTILIZATION PUBLICATIONS: Information on technology used by NASA that may be of particular interest in commercial and other non-aerospace applications. Publications include Tech Briefs, Technology Utilization Reports and Notes, and Technology Surveys.

Details on the availability of these publications may be obtained from:

SCIENTIFIC AND TECHNICAL INFORMATION DIVISION
NATIONAL AERONAUTICS AND SPACE ADMINISTRATION
Washington, D.C. 20546